



Derivation and conformity measurement of a popular explicit analytic Borowy 2C PV module model

Jianmin ZHANG (✉), Qianzhi ZHANG

Abstract A popular explicit analytic Borowy 2C PV module model is proposed for power generation prediction. The maximum power point and the open-circuit point which are calculated in this model cannot be equal to the data given by manufacturers under standard test condition (STC). The derivation of this model has never been mentioned in any literatures. The parameter forms of 2C model in this paper are more simplified, and the model is decomposed into a STC sub-model and an incremental sub-model. The STC model is derived successfully from an ideal single-diode circuit model. Relative error estimations are developed to do the conformity error measurements. The analysis results showed that though the biases at those critical points are very small, the conformity will depend on both of the two ratio values I_m/I_{sc} and V_m/V_{oc} , which can be used to verify whether 2C model is applicable for the PV module produced by a particular manufacturer.

Keywords Photovoltaic module, Analytic model, Explicit model, Implicit model, Borowy model, Conformity check, Derivation of the model, Conformity error measurement

CrossCheck date: 17 November 2014

Received: 9 April 2014 / Accepted: 24 November 2014 / Published online: 16 December 2014

© The Author(s) 2014. This article is published with open access at Springerlink.com

J. ZHANG, School of Automation, Hangzhou Dianzi University, Hangzhou 310017, China

(✉) e-mail: zhangjmhcn@hdu.edu.cn

Q. ZHANG, School of Electrical, Computer, and Energy Engineering, Ira A. Fulton Schools of Engineering, Arizona State University, Tempe, AZ 85287-5706, USA

e-mail: zhang.qianzhi@asu.edu

1 Introduction

Analytic photovoltaic module modeling with the parameters provided by PV module manufacturer is critical for PV plant sizing [1, 2], simulation [3], testing [4], PV plant monitoring [5, 6], dispatching [7], and energy management [8]. A very popular PV module model introduced by Borowy & Salameh [2] named 2C model proposed in this paper, has been heavily cited by 229 papers from Google and 66 papers from IEEE-Xplore database, with no derivation process. [3–6] have used 2C model in their works. All known that the awareness of strong theoretic based or data well driven modeling process is necessary for a user, therefore, this paper aims to fill the blank and present not only a detailed derivation but also a conformity study of 2C model.

In Sect. 2, the 2C model is introduced, which can be decomposed into a sub-model under standard test condition (STC) and an incremental sub-model. Two new parameter sets ($\gamma_{I_m}, \gamma_{V_m}$) and ($\sigma_{I_m}, \sigma_{V_m}$) are introduced to simplify the model and help the further derivation and conformity study. The contradictions of 2C model with manufacturer's datasheet have been explored in Sect. 3. In Sect. 4, 2C model under STC is derived from a single-diode circuit model. The conformity error measurements of 2C model with manufacturer's datasheet have been developed in Sect. 5. Finally conclusions are made in Sect. 6.

2 2C model and its decomposition

2.1 Basic formula

$$I = I_{SC} \left[1 - C_1 \left(\exp \left(\frac{V - \Delta V}{C_2 V_{OC}} \right) - 1 \right) \right] + \Delta I \quad (1)$$



$$C_1 = \left(1 - \frac{I_m}{I_{sc}}\right) \exp\left(-\frac{V_m}{C_2 V_{oc}}\right) \tag{2}$$

$$C_2 = \left(\frac{V_m}{V_{oc}} - 1\right) / \ln\left(1 - \frac{I_m}{I_{sc}}\right) \tag{3}$$

$$\Delta I = \alpha \frac{R}{R_{ref}} \Delta T + \left(\frac{R}{R_{ref}} - 1\right) I_{sc} \tag{4}$$

$$\Delta V = -\beta \Delta T - R_s \Delta I \tag{5}$$

$$\Delta T = T_c - T_{ref} \tag{6}$$

where R and T_c are the solar irradiance and module temperature, respectively. C_1 , C_2 , ΔI , ΔV and ΔT are intermediate variables; I_{sc} is the short circuit current; V_{oc} is the open circuit voltage; I_m is the current at maximum power; V_m is the voltage at maximum power; α is the short circuit current temperature correlation (%/°C or A/°C); β is the open circuit voltage temperature correlation (%/°C or V/°C); R_{ref} and T_{ref} are the references of solar irradiance and ambient temperature and $R_{ref} = 1 \text{ kW/m}^2$, $T_{ref} = 25 \text{ }^\circ\text{C}$, respectively; R_s is internal series resistance.

2.2 New direct forms of C_1 and C_2

Assuming two parameter sets:

$$\begin{cases} \frac{I_m}{I_{sc}} = \gamma_{I_m}, & \frac{V_m}{V_{oc}} = \gamma_{V_m} \\ 1 - \frac{I_m}{I_{sc}} = \sigma_{I_m}, & 1 - \frac{V_m}{V_{oc}} = \sigma_{V_m} \end{cases} \tag{7}$$

From (7), the equation is obtained as follows:

$$C_1 = (\sigma_{I_m})^{\frac{1}{\sigma_{V_m}}} \tag{8}$$

$$C_2 = -\frac{\sigma_{V_m}}{\ln \sigma_{I_m}} \tag{9}$$

It can be proved that:

$$C_2 = -\frac{1}{\ln C_1} \tag{10}$$

$$0 < \sigma_{I_m} < 1, \quad 0 < \sigma_{V_m} < 1 \tag{11}$$

$$0 < C_1 < 1 \tag{12}$$

2.3 Decompose 2C model into two sub-models

2C model can be decomposed into two sub-models, one is the model under STC, the other one is the incremental model

1) Under STC, $R = R_{ref}$, $T_c = T_{ref}$, $\Delta I = 0$, $\Delta V = 0$, $\Delta T = 0$. (1) will be written as follows:

$$I(V) = I_{sc} \left[1 - C_1 \left(\exp\left(\frac{V}{V_{oc} C_2}\right) - 1\right)\right] \tag{13}$$

$$V(I) = C_2 V_{oc} \ln \left[1 + \frac{1}{C_1} \left(1 - \frac{I}{I_{sc}}\right)\right] \tag{14}$$

2) With R and T_c changing in time, ΔI , ΔV and ΔT will also change according to (4)–(6).

$$\begin{cases} I^* = I - \Delta I \\ V^* = V - \Delta V \end{cases} \tag{15}$$

(1) will become as follows:

$$I^* = I_{sc} \left[1 - C_1 \left(\exp\left(\frac{V^*}{C_2 V_{oc}}\right) - 1\right)\right] \tag{16}$$

Even if R and T_c are not the reference values, the characteristic curves of I and V are still the same under STC, since the pattern of (13) is same with (16). (15) is a coordinate shift operation to transform (V, I) into (V^*, I^*) . (13) and (16) are both determined by I_{sc} , V_{oc} and C_1 , C_2 . Therefore, the parameter forms of C_1 and C_2 will determine 2C model not only for its STC model, but also for its incremental model.

3 Contradictions of 2C model under STC

3.1 2C model at $V = 0$ under STC

Assuming $I = I''_{sc}$ at $V = 0$, (16) can be written as:

$$I''_{sc} = I_{sc} \tag{17}$$

which means the short circuit point in model is exactly at the assumed short circuit point.

3.2 2C model at $V = V_m$ under STC

Assuming $I = I''_m$ at $V = V_m$, (16) can be written from (7, 8, 10) as:

$$I''_m = I_m + I_{sc} C_1 \tag{18}$$

From (18), the bias between $I = I''_m$ and I_m can be derived as:

$$\Delta I''_m = I''_m - I_m = I_{sc} C_1 > 0 \tag{19}$$

which means that the power point of the model (V_m, I''_m) always locates at the upper side of the maximum power point (V_m, I_m) provided by manufactory.

3.3 2C model at $I = I_m$ under STC

Assuming $V = V''_m$ at $I = I_m$, from (14), V''_m is given as:

$$V''_m = C_2 V_{oc} \ln \left[1 + \frac{1}{C_1} \left(1 - \frac{I_m}{I_{sc}}\right)\right] \tag{20}$$

Defining:

$$Z_2 = V''_m / V_m \tag{21}$$

From (8) and (9), (20) can be written as:

$$Z_2 = \ln\left(1 + \sigma_{I_m}^{1-\frac{1}{\sigma_{V_m}}}\right) / \ln\left(\sigma_{I_m}^{1-\frac{1}{\sigma_{V_m}}}\right) \tag{22}$$

Defining:

$$x_3 = \sigma_{I_m}^{1-\frac{1}{\sigma_{V_m}}} \tag{23}$$

Thus:

$$z_2 = \ln(1 + x_3) / \ln(x_3) \tag{24}$$

(23) can be derived as:

$$\ln(x_3) = \left(1 - \frac{1}{\sigma_{V_m}}\right) \ln(\sigma_{I_m}) \tag{25}$$

From (11), it can be derived that

$$\left(1 - \frac{1}{\sigma_{V_m}}\right) < 0, \quad \ln(\sigma_{I_m}) < 0 \tag{26}$$

$$\ln(x_3) > 0 \tag{27}$$

which means $X_3 > 1$, $(1 + X_3)/X_3 > 1$, so that $\ln[(1 + X_3)/X_3] > 0$, $\ln(1 + X_3) - \ln(X_3) > 0$. Finally, it can be derived that

$$\ln(1 + x_3) > \ln(x_3) \tag{28}$$

(28) can be expressed as:

$$\ln(1 + x_3) / \ln(x_3) > 1 \tag{29}$$

Substituting (29) into (24), it is shown that $Z_2 > 1$, so that $V_m'' > V_m$ at $I = I_m$, i.e., the power point (V_m'', I_m) of the model always locates at the right side of the maximum power point (V_m, I_m) provided by manufactory.

3.4 2C model at $V = V_{oc}$ under STC

Assuming $I = I_0''$ at $V = V_{oc}$, (13) can be written from (8) and (9) as:

$$I_0'' = I_{sc} \left[1 - \sigma_{I_m}^{\frac{1}{\sigma_{V_m}}} \left(\sigma_{I_m}^{\frac{-V_{oc}}{V_{oc}\sigma_{V_m}}} - 1 \right) \right] = I_{sc} \sigma_{I_m}^{\frac{1}{\sigma_{V_m}}} = I_{sc} C_1 > 0 \tag{30}$$

which means the current at $V = V_{oc}$ is greater than 0, with a constant error $I_{sc} C_1$.

4 A derivation of C_1 and C_2 from an ideal single-diode PV circuit model

4.1 PV circuit model with an ideal single-diode

The circuit model based on semiconductor theory with a single diode is given by (1) [9].

$$I = I_{ph} - I_s \left[\exp\left(\frac{q(V + R_s I)}{nkT}\right) - 1 \right] - \frac{V + R_s I}{R_{sh}} \tag{31}$$

where I_{ph} is the photonic current (principally depends on the solar irradiance); I_{s1} and I_{s2} are the reverse saturation currents of diode 1 and 2, respectively; q is the electron charge and $q = 1.60,217,646 \times 10^{-19}$ C; k is the Boltzmann constant and $k = 1.3,806,503 \times 10^{-23}$ J/K; T is the cell temperature in Kelvin; n is the diode ideality factors; R_s is the series resistance; R_{sh} is the shunt resistance. (31) is a complex equation without any explicit solutions for both voltage V and current I .

If neglecting R_s and R_{sh} , (1) will become:

$$I(V) = I_{ph} - I_s = I_{ph} - I_0 \left[\exp\left(\frac{V}{V_T}\right) - 1 \right] \tag{32}$$

where I_0 is the reverse saturation current; V_T is the energy equivalent [9].

At the short circuit point under STC, (32) becomes:

$$I(V)|_{V=0} = I_{ph} = I_{sc} \tag{33}$$

Thus:

$$I(V) = I_{sc} - I_0 \left[\exp\left(\frac{V}{V_T}\right) - 1 \right] \tag{34}$$

(14) can be expressed as:

$$V(I) = V_T \ln \left[1 + \left(\frac{I_{sc} - I}{I_0} \right) \right] \tag{35}$$

It is known that when $I = I_{sc} - I_0(e - 1)$, the observed voltage is equal to V_T , which can be expressed as follows:

$$V_T = V(I)|_{I=I_{sc}-I_0(e-1)} \tag{36}$$

4.2 A single-diode PV circuit model expressed by C_1 and C_2

Substituting (34) into the following form:

$$I(V) = I_{sc} \left\{ 1 - \frac{I_0}{I_{sc}} \left[\exp\left(\frac{V_{oc}}{V_T} \cdot \frac{V}{V_{oc}}\right) - 1 \right] \right\} \tag{37}$$

Assuming there are two new parameters C_1^* and C_2^* , which are expressed as:

$$C_1^* = \frac{I_0}{I_{sc}}, \quad C_2^* = \frac{V_T}{V_{oc}} \tag{38}$$

(37) can be derived as:

$$I(V) = I_{sc} \left\{ 1 - C_1^* \left[\exp\left(\frac{V}{C_2^* V_{oc}}\right) - 1 \right] \right\} \tag{39}$$

4.3 Key equation to solve C_1^* and C_2^*

C_1^* and C_2^* can be derived by (39) at the open circuit point and MPP points.



1) At the open circuit point, assuming $V = V_{oc}, I = 0$, (39) can be derived as:

$$\exp\left(\frac{1}{C_2^*}\right) = 1 + \frac{1}{C_1^*} \tag{40}$$

For simplifying, defining

$$\begin{cases} C_3 = 1/C_1^* \\ C_4 = 1/C_2^* \end{cases} \tag{41}$$

(40) can be expressed as:

$$\exp(C_4) = 1 + C_3 \tag{42}$$

2) At the MPP point, assuming $V = V_m, I = I_m$, (38) can be derived as:

$$1 + (1 - \gamma_{I_m})C_3 = (1 + C_3)^{\gamma_{V_m}} \tag{43}$$

Defining

$$y = 1 + (1 - \gamma_{I_m})C_3 - (1 + C_3)^{\gamma_{V_m}} \tag{44}$$

which is the key equation to get the solution of C_3 when $y = 0$. The curve of (44) is shown in Fig. 1.

4.4 Solution of C_1^* and C_2^*

Normally, $C_3 \gg 1$ when $\gamma_{I_m} \in [0.85, 0.99]$; $\gamma_{V_m} \in [0.75, 0.85]$ [10]. Thus:

$$1 + C_3 \cong C_3 \tag{45}$$

(43) can be expressed by C_1^* according to (41) as:

$$C_1^* \left[C_1^* - \left(1 - \frac{I_m}{I_{SC}}\right) \left(\frac{1}{1 - \frac{V_m}{V_{OC}}}\right) \right] = 0 \tag{46}$$

Since $C_3 \gg 1, C_1^* \neq 0$, the final solution is given by

$$C_1^* = \left(1 - \frac{I_m}{I_{SC}}\right) \left(\frac{1}{1 - \frac{V_m}{V_{OC}}}\right) \tag{47}$$

which is same with C_1 in direct form given by (8), proving the indirect form given by (2). From (45), (42) can be written as:

$$\exp(C_4) = C_3 \tag{48}$$

Thus

$$C_2^* = (C_4^*)^{-1} = (\ln C_3)^{-1} = \left(\frac{V_m}{V_{OC}} - 1\right) / \ln\left(1 - \frac{I_m}{I_{SC}}\right) \tag{49}$$

which is also exactly the same with (3).

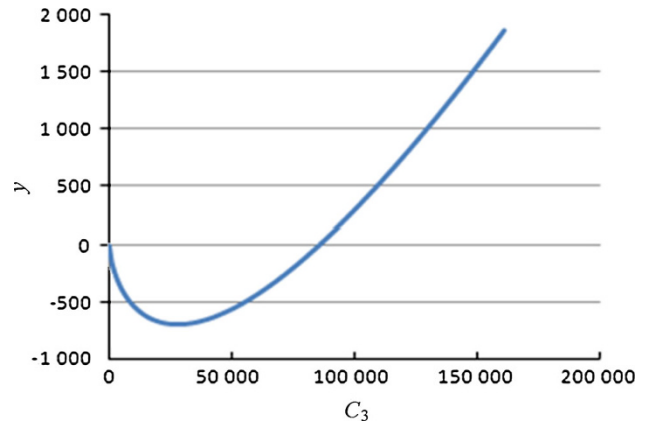


Fig. 1 Curve of (44)

4.5 I_0 and V_T in generic single-diode PV circuit model

According to (39) and (7), I_0 and V_T are given by

$$I_0 = C_1^* I_{sc} = I_{sc} (\sigma_{I_m})^{\frac{1}{\sigma_{V_m}}} \tag{50}$$

$$V_T = C_2^* V_{oc} = -V_{oc} (\sigma_{V_m}) / (\ln \sigma_{I_m}) \tag{51}$$

5 The conformity measurement of STC sub-model calculated data with manufacturer's datasheet

5.1 The error of the calculated maximum voltage in model and the provided maximum voltage

According to (20), the relative error is defined as:

$$\delta_{V_{oc}} = \frac{V''_{oc} - V_{OC}}{V_{OC}} = \frac{V''_{oc}}{V_{OC}} - 1 = C_2 \ln\left(1 + \frac{1}{C_1}\right) - 1 \tag{52}$$

$$= -(\ln C_1)^{-1} \ln(1 + C_1^{-1}) - 1 \tag{53}$$

It is known that $\delta_{V_{oc}}$ is greater than 0 since C_1 is great than 0 from Fig. 2.

At the open-circuit point, V_{oc} calculated in 2C STC sub-model is greater than the the assumed value one, and the bias $\delta_{V_{oc}}$ greatly depends on the value of C_1 . The bias will increase if C_1 increases.

Replacing C_1 by γ_{I_m} and γ_{V_m} into (53),

$$\delta_{V_{oc}} = -\frac{(1 - \gamma_{V_m}) \ln\left(1 + 1 / (1 - \gamma_{I_m})^{1/(1 - \gamma_{V_m})}\right)}{\ln(1 - \gamma_{I_m}) - 1} \tag{54}$$

Fig. 3 shows that $\delta_{V_{oc}} \in [1.78e^{-15}, 6.67e^{-5}]$ when $\gamma_{I_m} \in [0.85, 0.99]$, $\gamma_{V_m} \in [0.75, 0.85]$. The error of the maximum voltage V'_{oc} which is calculated with the maximum

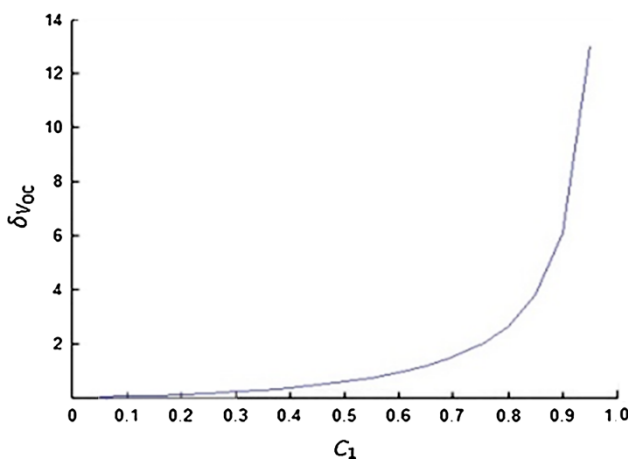


Fig. 2 Curve of (53)

voltage V_{oc} provided by manufactory is very small though $V'_{oc} > V_{oc}$.

5.2 The error of between I''_m and I_m at $V = V_m$ under STC

From (18) and (12), the relative error is given as:

$$\delta_{I_m} = \frac{\Delta I''_m}{I_m} = \frac{I''_m - I_m}{I_m} = \frac{I_{SC}}{I_m} C_1 > 0 \tag{55}$$

$$= \frac{1}{\gamma_{I_m}} (1 - \gamma_{I_m})^{1/(1-\gamma_{V_m})} \tag{56}$$

From Fig. 4, it is shown that $\delta_{I_m} \in [4.69e^{-14}, 5.96e^{-4}]$ when $\gamma_{I_m} \in [0.85, 0.99]$, $\gamma_{V_m} \in [0.75, 0.85]$. The error of I''_m at $V = V_m$ and I_m at the MPP point is very small though $I''_m > I_m$

5.3 The error between V''_m and V_m at $I = I_m$ under STC

From (20) and (7), it can be obtained that:

$$\delta_{V_m} = -\frac{(1 - \gamma_{V_m})}{\gamma_{V_m} \ln(1 - \gamma_{I_m})} \ln \left[1 + (1 - \gamma_{I_m}) \left(\frac{\gamma_{V_m}}{1 - \gamma_{V_m}} \right) \right] \tag{57}$$

In Fig. 5, $\delta_{V_m} \in [1.78e^{-13}, 5.92e^{-4}]$ when $\gamma_{I_m} \in [0.85, 0.99]$, $\gamma_{V_m} \in [0.75, 0.85]$, which means the error between V''_m and V_m at the MPP point is very small though $V''_m > V_m$.

5.4 Prove of $V_m < V'_m < V''_m$ and $I_m < I'_m < I''_m$

dP/dV is decreasing monotonously and it is 0 at point (V'_m, I'_m) . If dP/dV at point (V_m, I''_m) is greater than 0, and

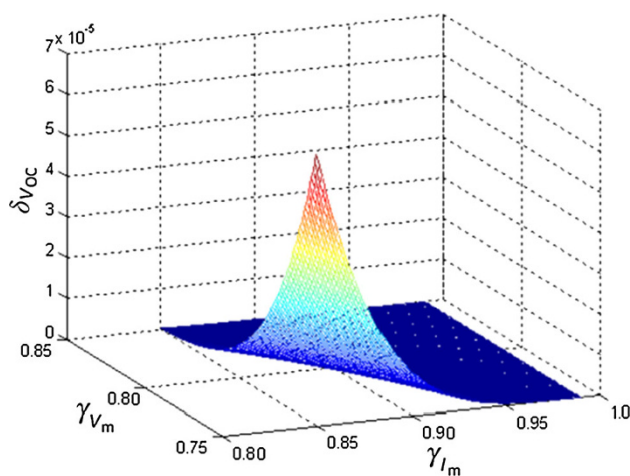


Fig. 3 Relative error $\delta_{V_{oc}}$ with γ_{I_m} and γ_{V_m} in (54)

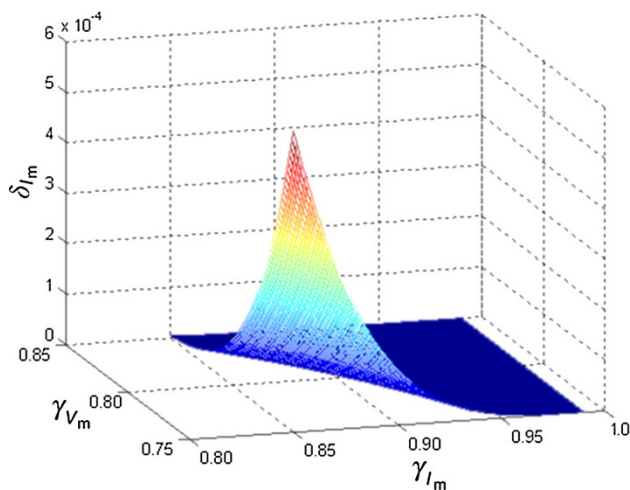


Fig. 4 Relative error δ_{I_m} with γ_{I_m} and γ_{V_m} in (56)

dP/dV at (V''_m, I_m) is smaller than 0, the above non-equality can be proved.

$$\frac{dP}{dV} = I_{SC} \left[\frac{I}{I_{SC}} - \frac{V}{C_2 V_{oc}} \left(1 + C_1 - \frac{I}{I_{SC}} \right) \right] \tag{58}$$

At point (V_m, I''_m) ,

$$\begin{aligned} \frac{dP}{dV} \Big|_{(V_m, I''_m)} &= I_{SC} \left[\left(C_1 + \frac{I_m}{I_{SC}} \right) - \frac{V_m}{C_2 V_{oc}} \left(1 - \frac{I_m}{I_{SC}} \right) \right] \\ &= I_{SC} \left\{ 1 + (1 - \gamma_{I_m}) \left[(1 - \gamma_{I_m}) \left(\frac{\gamma_{V_m}}{1 - \gamma_{V_m}} \right) - 1 \right. \right. \\ &\quad \left. \left. - \frac{\gamma_{V_m}}{1 - \gamma_{V_m}} \ln(1 - \gamma_{I_m}) \right] \right\} \end{aligned} \tag{59}$$

From Fig. 6, dP/dV is greater than 0 when $\gamma_{I_m} \in [0.85, 0.99]$, $\gamma_{V_m} \in [0.75, 0.85]$.



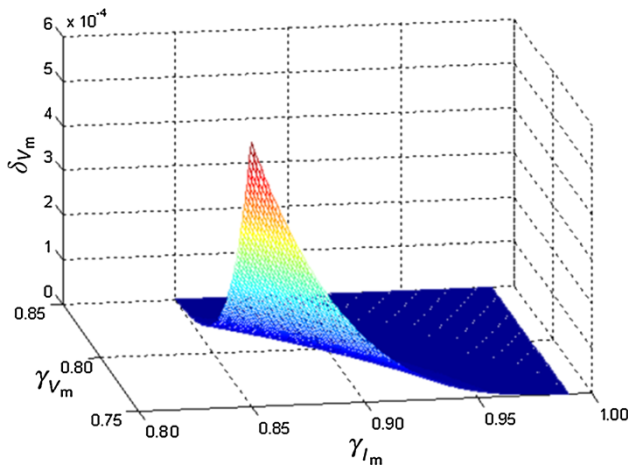


Fig. 5 Relative error δ_{V_m} with $\gamma_{I_m}, \gamma_{V_m}$ and in (57)

From (17), it can be derived that

$$V_m'' = C_2 V_{OC} \ln \left[1 + \frac{1}{C_1} \left(1 - \frac{I_m}{I_{SC}} \right) \right]$$

$$= C_2 V_{OC} \ln \left[1 + \frac{1}{C_1} (1 - \gamma_{I_m}) \right] \tag{60}$$

Then (58) can be expressed as:

$$\frac{dP}{dV} \Big|_{(V_m'', I_m)} = I_{SC} \left\{ 1 - (1 - \gamma_{I_m}) \left\{ 1 + \left[1 + \left(1 + (1 - \gamma_{I_m})^{\frac{\gamma_{V_m}}{1 - \gamma_{V_m}}} \right) \right] \right\} \right\}$$

$$\times \ln \left(1 + (1 - \gamma_{I_m})^{\frac{-\gamma_{V_m}}{1 - \gamma_{V_m}}} \right) \tag{61}$$

The value of dP/dV at point (V_m'', I_m) is smaller than 0 when when $\gamma_{I_m} \in [0.85, 0.99]$, $\gamma_{V_m} \in [0.75, 0.85]$ in Fig. 7.

5.5 The error between the maximum power calculated in model and provided by manufactory

Defining the voltage and current at the MPP point are V_m' and $I_m' P_m = V_m I_m$, the error can be given as:

$$\delta_{P_m} = \frac{\Delta P}{P_m} = \frac{P_m' - P_m}{P_m} = (1 + C_1) \frac{I_{SC} V_m'}{I_m V_m} - C_2 \frac{I_m' V_{OC}}{I_m V_m} - 1 \tag{62}$$

It is difficult to have an explicit expression of δ_{P_m} . It is proved above that

$$V_m < V_m'' < V_m', I_m < I_m'' < I_m' \tag{63}$$

From (56) and (57), it is derived that

$$\frac{I_m''}{I_m} = \delta_{I_m} + 1 < \max(\delta_{I_m}) + 1 = 1.000,596 \tag{64}$$

$$\frac{V_m''}{V_m} = \delta_{V_m} + 1 < \max(\delta_{V_m}) + 1 = 1.000,592 \tag{65}$$

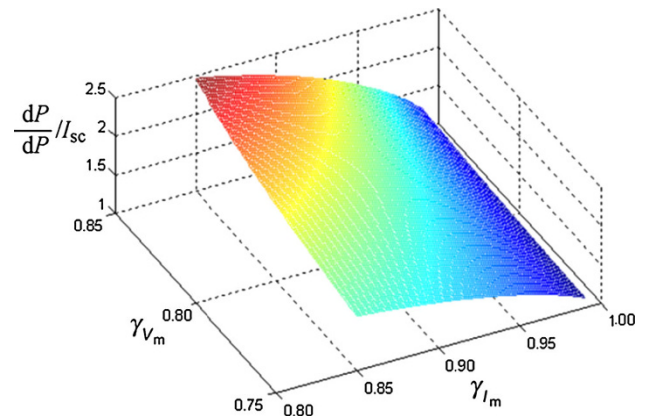


Fig. 6 Curve of dP/dV at point (V_m, I_m'') in (59)

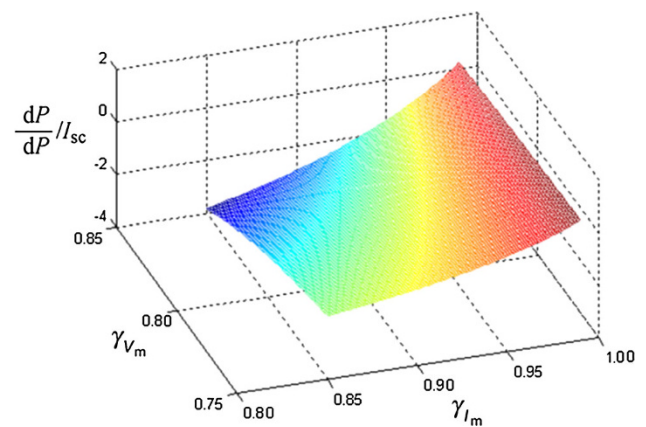


Fig. 7 Curve of dP/dV at point (V_m'', I_m) in (61)

Thus:

$$\delta_{P_m} = \frac{\Delta P}{P_m} = \frac{P_m''}{P_m} - 1 = \frac{I_m' V_m'}{I_m V_m} - 1 < \frac{I_m'' V_m''}{I_m V_m} - 1$$

$$< (\max(\delta_{V_m}) + 1)(\max(\delta_{I_m}) + 1) - 1$$

$$= 1.000,596 * 1.000,592 - 1 = 0.001,19 = 0.119\% \tag{66}$$

which means the model relative error of the calculated maximum power is small and negligible.

6 Conclusion

1) 2C model is a single-diode circuit model, since it can be derived to a single-diode circuit model theoretically. (39) defines the original physical parameters of 2C, i.e., C_1 is the ratio of reverse saturation current I_0 to the short circuit current I_{sc} , C_2 is the ratio of energy equivalent V_T to the open circuit voltage V_{oc} .

2) The expressions of C_1 and C_2 in manufacturer's datasheet of 2C model are mostly correct under a reasonable approximation assumption for almost manufacturer's PV modules.

3) Though there are contradictions of 2C model with manufacturer's datasheet, the relative errors are very small, which can be negligible in engineering application.

4) The conformity error measurement method by 3D curves gives a systematic method for power community users to be aware of the conformity errors of their own PV modules by using 2C model in real application.

Therefore, the calculate data in 2C model is almost the same with the manufacturer's datasheet under STC. If applying 2C model in a real application, it is necessary to find other PV module models.

Acknowledgement This work was partially supported by Key Science, Technology Project of Zhejiang Province (LZ12E07001) and National Natural Science Foundation of China (51307038).

Open Access This article is distributed under the terms of the Creative Commons Attribution License which permits any use, distribution, and reproduction in any medium, provided the original author(s) and the source are credited.

References

- [1] Borowy BS, Salameh ZM (1994) Optimum photovoltaic array size for a hybrid wind/PV system. *IEEE Trans Energy Convers* 9(3):482–488
- [2] Borowy BS, Salameh ZM (1996) Methodology for optimally sizing the combination of a battery bank and PV array in a Wind/PV hybrid system. *IEEE Trans Energy Convers* 11(2): 367–375
- [3] Mao MQ, Yu SJ, Su JH (2005) Versatile Matlab simulation model for photovoltaic array with MPPT function. *J Syst Simul* 17(5):1248–1251 (in Chinese)
- [4] Mao MQ, Su JH, Chang LC et al (2009) Research and development of fast field tester for characteristics of solar array. In: Proceedings of the Canadian conference on electrical and computer engineering (CCECE'09), St John's, 3–6 May 2009, pp 1055–1060
- [5] Zhang JM, Zhang QZ, Wang N et al (2011) Power generation model and its parameter calibration for grid-connected photovoltaic power plant energy data acquisition and supervisory system. *Automat Electr Power Syst* 35(13):22–26 (in Chinese)
- [6] Zhang QZ, Zhang JM, Guo CX (2012) Photovoltaic plant metering monitoring model and its calibration and parameter assessment. In: Proceedings of the 2012 IEEE Power and Energy Society general meeting, San Diego, 22–26 July 2012, 7 pp
- [7] Han XN, Ai X, Sun YY (2014) Research on large-scale dispatchable grid-connected PV systems. *J Mod Power Syst Clean Energy* 2(1):69–76 (in Chinese)
- [8] Li YW, Nejabatkhah F (2014) Overview of control, integration and energy management of microgrids. *J Mod Power Syst Clean Energy* 2(3):212–222 (in Chinese)
- [9] Masters GM (2004) Renewable and efficient electric power systems. Wiley, Hoboken
- [10] Download solar panel datasheets. <http://eng.sfe-solar.com/download-photovoltaic-datasheets/>

Jianmin ZHANG received B.Sc. degree and M.Sc. degree from Huazhong University of Science and Technology (HUST), China, in 1984 and 1987, respectively. He received M.E. degree from Indian Institute of Technology (IIT, Roorkee) in electrical engineering in 1992. He joined Hangzhou Regional Center of Small Hydro Power (HRC) and National Institute of Rural Electrification, China, from 1987 to 1997. He is a full professor and academic leader of Electrical Engineering and Automation at Hangzhou Dianzi University. His research interests include electric power and energy system modeling, optimal operation and dispatching, intelligence engineering and automation and information system integration.

Qianzhi ZHANG received B.Sc. degree in electrical engineering from Shandong University of Technology in 2012. Presently he is a research assistant, pursuing master science of electrical engineering, in Ira A. Fulton Schools of Engineering, Arizona State University. His research interests include the renewable energy integration with power system and their planning, design, control and operation.

